

## PHOTOCATALYTIC OZONATION FOR THE DEGRADATION OF TETRADIFON PESTICIDE ON Mn/TiO<sub>2</sub> UNDER VISIBLE LIGHT

**MADDILA S.\*, OSEGHE E.O., PALAKONDU L. and JONNALAGADDA S.B.**

<sup>1</sup>School of Chemistry, University of KwaZulu-Natal, Westville campus, Chiltern Hills, Durban-4000, South Africa, <sup>2</sup>Department of Chemistry, Annamacharya Institute of Technology & Sciences, J.N.T.University, Tirupati -517 502, Andhra Pradesh, India.  
E-mail: sureshmskt@gmail.com

### ABSTRACT

The photocatalytic activity of Mn doped TiO<sub>2</sub> for the ozonation of tetradifon pesticide in aqueous solution was studied. Various loadings of catalysts Mn/TiO<sub>2</sub> (1%, 2.5% and 5%) was prepared and characterized by standard analytical techniques. Photocatalyzed ozonation with 2.5% Mn/TiO<sub>2</sub> yielded 100% degradation and mineralization of tetradifon in 2.0 h under basic pH conditions. The extent of degradation of tetradifon pesticide and its mineralization were confirmed by GC-MS. For 10 mg/L of tetradifon, 0.1 g L<sup>-1</sup> of catalyst was found to be the optimum for effective mineralisation. The reused experiment confirmed that Mn/TiO<sub>2</sub> kept a good photocatalytic activity and stability, and it was a promising heterogeneous catalyst. The catalyst is fully recoverable and reusable multiple times with no loss of activity.

**Keywords:** Tetradifon; Advanced Oxidation; Photocatalyst; Mn/TiO<sub>2</sub>; Degradation.

### 1. Introduction

In recent times Tetradifon (pesticide) has globally applied as insecticides in agriculture, and in the synthesis of industrial and medicinal products [1]. Due to its high toxicity, persistence, and bioaccumulative properties they have become treat to the environment [2]. Therefore, the control of organic pollutants in water is an important measure in environmental protection. Lately, considerable attention has been focused on the degradation of pesticides via photocatalytic ozonation [3].

Heterogeneous photocatalytic ozonation has received great attention due to its high oxidation potential that originates from the formation of hydroxyl radicals as well as a lack of secondary pollutants generation compared with the homogeneous catalytic process [4]. In this process, the presence of the heterogeneous catalyst surfaces induces the decomposition of ozone, and subsequently generates the hydroxyl radicals. As significant functional materials in solid catalysts, manganese loaded titania have been commonly employed because of their stability and abundance in nature, as well as their higher catalytic efficiency during the photocatalytic ozonation process. Our group has proved that photocatalytic ozonation with Mn doped TiO<sub>2</sub> improves the degradation and mineralization of pesticide.

### 2. Materials and method

#### 2.1 Photocatalytic Ozonolysis Experiment

For photoozone generation, The light source was a 500-W xenon lamp (CHFXQ500 W) with a UV filter that can cut off UV light with wavelengths shorter than 420 nm and a Fischer Ozone 500 generator was used. Ozone enriched oxygen stream was passed through a sintered glass (porosity 2) into the 50 cm<sup>3</sup> reactor at a flow rate of 10 mL per min. The reactor temperature was maintained at (19 ± 1) °C by circulating water through double walled jacket. For each run, 20 mL 10 % w/v of Tetradifon and fixed ozone concentration (0.05 M) and flow rate of 10 mL/min. A magnetic stirrer was used to ensure continuous mixing. Ozone concentration in oxygen stream was determined using KI method [5,6]. Before and after each of the experiment the flow rate and photoozone content were monitored in duplicate runs.

## 2.2. Catalyst preparation

The photocatalysts were prepared by deposition-precipitation method by impregnating Mn over titania. 1.6 g of TiO<sub>2</sub> was suspended in 60 mL of deionized water under vigorous stirring for 30 min. Then, 1.8 ml of 0.2 M manganese nitrate aqueous solution (Mn(NO<sub>3</sub>)<sub>2</sub>, Aldrich, 99.98 % trace metals basis) was added. This solution was preserved unstirred for 1.0 h. Then the manganese aqueous solution was added slowly into the TiO<sub>2</sub> suspension under stirring. For the completion of addition, the pH was adjusted to 11 using 0.1 M NaOH solution. The suspension was vigorously stirred for another 2 h. The precipitate was aged at 60-70 °C for 2 h in the mother solution. Then the precipitate was filtered and washed with deionized water for three times. The samples were dried at 110-120 °C for overnight and then calcined in the presence of air, at 450 °C for 4 h to obtain the 1.0%, 2.5%, and 5.0% w/w of Mn/TiO<sub>2</sub> catalysts.

## 2.3. Instrumentation

All the catalyst characterization and product identification was achieved adopting the following techniques: PXRD, SEM-EDX, TEM, N<sub>2</sub> sorption, ICP, PL, FTIR, GC-MS, <sup>1</sup>H NMR spectral analysis [6-8].

## 3. Results and discussion

### 3.1. BET Surface and elemental analysis

The N<sub>2</sub> sorption study was carried out over bare TiO<sub>2</sub> and Mn doped TiO<sub>2</sub> catalysts (Figure. 1). N<sub>2</sub> sorption resulted in typical type IV isotherm, with a H2 hysteresis loop. The BET surface areas of bare TiO<sub>2</sub> and Mn/TiO<sub>2</sub> catalysts were found to be 38.45 and 79.82 m<sup>2</sup> g<sup>-1</sup>, respectively. It is evident from these results that there was a significant change in the surface area from the TiO<sub>2</sub> to Mn doped TiO<sub>2</sub> catalyst. Table-1 summarizes the obtained BET surface area, pore diameter and pore volume.

**Table 1:** BET surface area, elemental analysis and band-gap of Mn loaded supports

Catalyst	Mn Wt% (From ICP)	Surface Area (m <sup>2</sup> /g)	Pore volume (cm <sup>3</sup> /g)	Mn wt % (From EDX)	Band-gap Energy (eV)
Bare TiO <sub>2</sub>	—	38.45	0.24	—	3.20
1.0 % Mn-TiO <sub>2</sub>	0.98	51.66	0.16	0.98	3.10
2.5 % Mn-TiO <sub>2</sub>	2.46	64.48	0.14	2.48	2.84
5.0 % Mn-TiO <sub>2</sub>	4.98	79.82	0.10	4.97	2.76

### 3.2. SEM and TEM

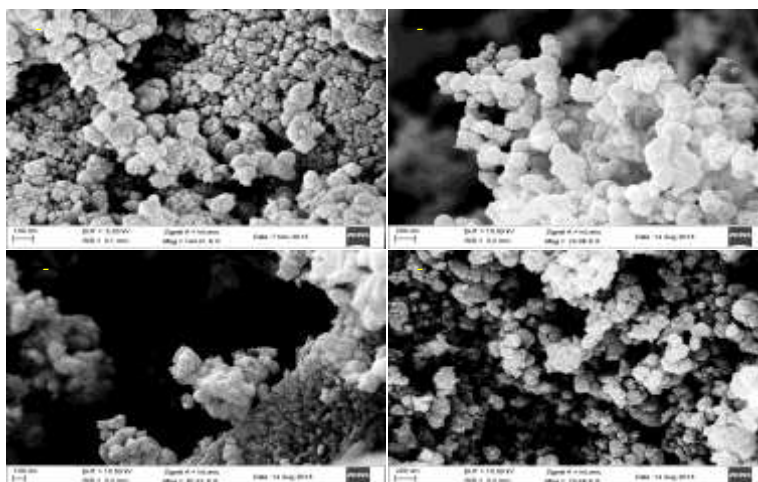


**Figure 1S:** SEM images of (a) Bare TiO<sub>2</sub> (b) 1% Mn/TiO<sub>2</sub> (c) 2.5% Mn/TiO<sub>2</sub> (d) 5% Mn/TiO<sub>2</sub>

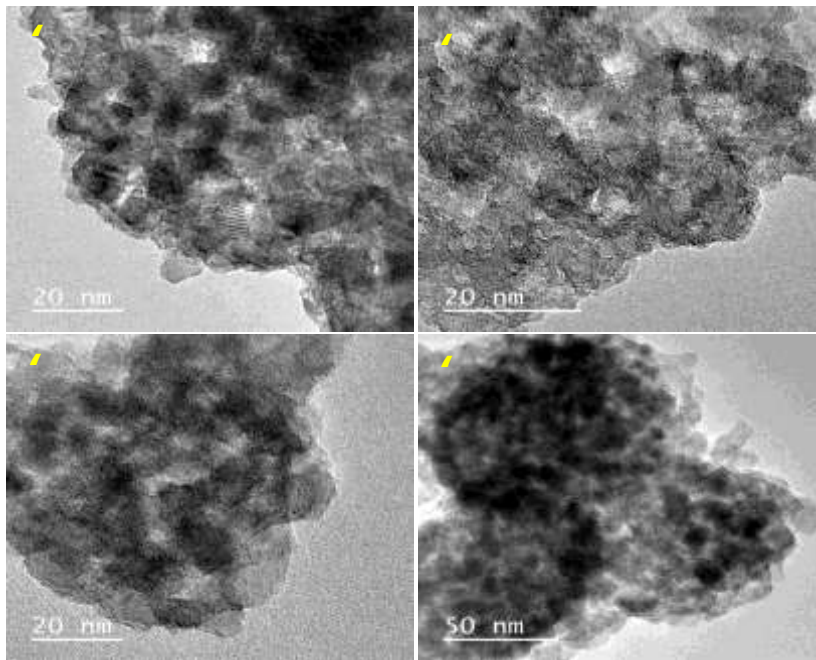


**Figure 2S:** TEM images of (a) Bare TiO<sub>2</sub> (b) 1% Mn/TiO<sub>2</sub> (c) 2.5% Mn/TiO<sub>2</sub> (d) 5% Mn/TiO<sub>2</sub>

The morphology of bare and Mn doped titania (1%, 2.5% & 5.0%) catalysts were examined by scanning electron microscopy; the images obtained are presented in Figure 1S. a-d respectively. The SEM images of bare titania and Mn doped titania at various amplifications display the partial crystalline nature. The surface morphology of titania appears to be changed after Mn loading. The EDX analysis evidently specifies the presence of Mn species on the surface of titania. The TEM images of the undoped and doped titania calcined catalysts and used are shown in Figure 2S. a-d. In these catalysts, the concentration of Mn increases average particle size decreases and the agglomeration between the particles also reduces.

### 3.3. XRD analysis

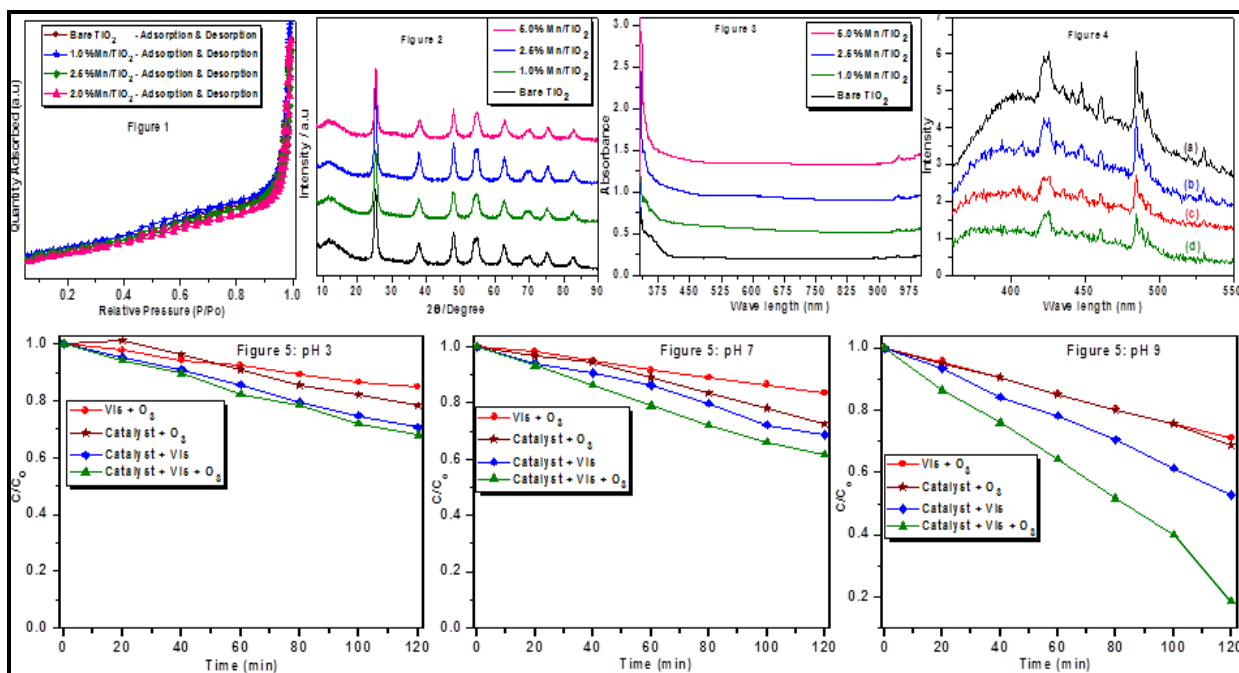
Figure 2 shows the XRD diffraction patterns of bare titania and Mn doped titania (1%, 2.5% and 5%) powder samples calcined at 450 °C. The diffractograms indicates peaks which corresponds to 2θ values of 25.3° for (1 0 1), 37.8° for (0 0 4) and 47.9° (2 0 0) (JCPDS file no. 21-1272) and are typical for anatase phase.

### 3.4. UV-DRS:

UV-diffuse reflectance spectra of titania and various (% w/w) Mn loaded titania catalysts are acquired in Figure. 3. TiO<sub>2</sub> has a strong absorption band at approximately 384 nm corresponding to band-gap energy of 3.2 eV calculated from the formula  $k = 1239.8/E_{bg}$  (Table 1S). On doping with Mn, a red-shift was observed which could foster the photocatalytic activities of the catalyst under visible light.

### 3.5. Photoluminescence Spectra

Figure 4 shows the PL spectra of samples in the range of 350–500 nm with the excitation wavelength of 360 nm. The PL spectra might be closely related to the recombination of photo-induced electrons and holes, and free and self-trapped excitons, which possibly generate from surface defects in the TiO<sub>2</sub> crystals, such as lattice distortions and surface oxygen deficiencies



[9]. The spectra show that the intensity of the Mn doped titania was decreased as compared to the bare titania, which indicates the reduction of the recombination centers for the electrons and holes in the samples. This describes that the Mn doped titania may have low electron-holes recombination rate under light irradiation and may show better photocatalytic activity than bare TiO<sub>2</sub>.

### 3.6. Effect of pH

The influence of pH on the effectiveness of tetracycline degradation by ozonation is shown in Figure. 5. The degradation experiments were carried out at pH values of 3, 7 and 11. The degradation rate increased as the pH increased from 3 to 11. Under acidic pH, O<sub>3</sub> molecule is main reactive species and its reactivity is very low relative to hydroxyl radical, so the degradation of tetracycline very low. As the solution becomes more basic, the rate of photocatalyzed decomposition of ozone to secondary oxidants, such as hydroxyl radicals increases. While the increase in pH facilitates the hydroxyl radical concentration, the effect of pH on the substrate reactivity is also equally vital for efficient conversion. The obtained results indicate that the process effectiveness increases significantly and highest conversion was recorded at pH 11.

### 3.7. Effect of catalyst concentration

The effects of catalyst concentration on the tetracycline photodegradation, It is observed from Figure. 3S.

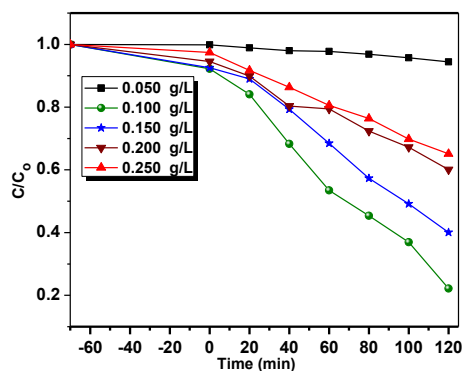


Figure 3S: Effect of Mn/TiO<sub>2</sub> catalyst concentration at pH 11

The photocatalytic efficiency of the tetradifon samples increases up to the catalyst concentration of 0.05 to 0.250 g L<sup>-1</sup>, for the tetradifon photooxidation. The optimum weight of catalyst loading was found to be 0.1 g L<sup>-1</sup>. Further increase in catalyst weight resulted in the decrease of the reaction rate. This can be explained in terms of availability of active sites on the catalyst surface and the penetration of visible light into the suspension. The total active surface area increases with increasing catalyst weight but at the catalyst weight above optimum loading decrease in visible light penetration may be due to screening effect of excess catalyst particle in the solution. Hence, the initial rate decreases at the higher catalyst loading.

### 3.8. Effect of Mn doping concentrations

Photo induced oxidation of tetradifon in the presence of the bare TiO<sub>2</sub> and Mn on titania was carried out in order to study the photocatalytic activity under visible light. The photocatalytic activity of Mn/TiO<sub>2</sub> photocatalyst was significantly enhanced on the addition of Mn loading. Additionally, the photocatalytic activity of Mn doped titania increased with the increasing doping concentration of Mn (1 to 5.0%). An increase in the amount of Mn dopant resulted in the increasing visible light absorption and hence enhanced photocatalytic activity. The optimal tetradifon degradation was found to be at 5 wt.% Mn concentration with the removal efficiency.

### 3.9. Catalyst testing and product identification

All the photocatalyzed ozonation experiments were accompanied by exposing the reaction mixtures with visible light and with a flow of ozone enriched oxygen. After ozone aeration, the organic portion of the reaction mixture was extracted and analyzed after every reaction with 20 min intervals. The six products identified by GC-MS (Figure. 4S). The peaks from 8.00-17.00 retention times refer to the intermediates and various carboxylic acid compounds formed due to the further oxidation of the products of the reaction. The peaks at retention time 8.507, 9.709, 11.401, 13.558, 15.807 and 16.658 minutes refer to the compounds of (a) oxalic acid (OA), (b) trichlorobenzene (TCB), (c) fumaric acid (FA), (d) dihydroxyhexa-2,4-dienedioic acid (DHDDA), (e) 4-chlorobenzenesulfonic acid (CBSA), and (f) 3-hydroxyhexa-2,4-dienedioic acid (HDDA) respectively. Furthermore, the formation of these products was confirmed by GC-MS with their respective (M<sup>+</sup>) m/z values (Figure. 5S a-f). The peaks observed in <sup>1</sup>H-NMR and FT-IR spectra of the products were in good agreement with spectra of the functional groups present in the products. Additionally, the qualitative lime water test confirmed the release of CO<sub>2</sub> during the reactions and suggested some mineralization of pesticides. Photo catalytic ozonation of pesticides in water is known to produce more biodegradable oxygenated organic products and low molecular weight acids.

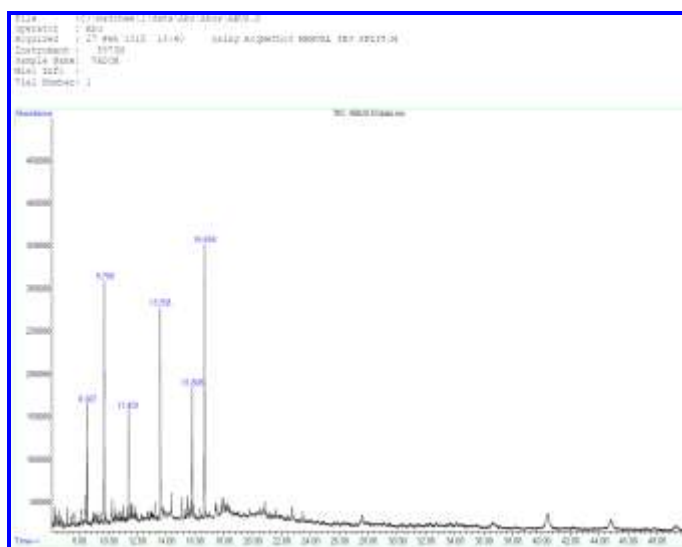


Figure 4S: GC-MS chromatogram of product mixture



Figure 5s: (a) GC-MS Mass Spectrum of the OA

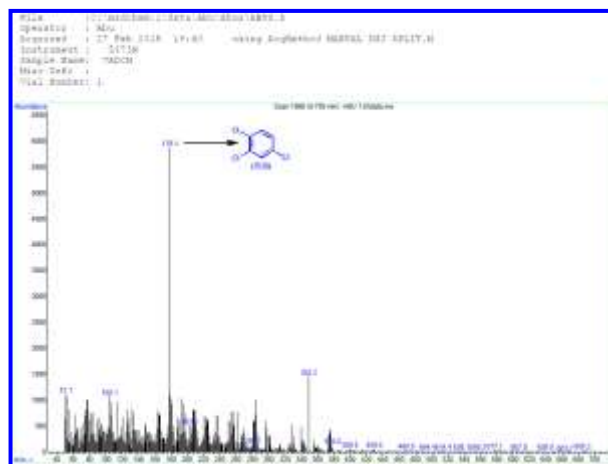


Figure 5s: (b) GC-MS Mass Spectrum of the TCB



Figure 5s: (c) GC-MS Mass Spectrum of the FA



Figure 5s: (d) GC-MS Mass Spectrum of the DHDDA



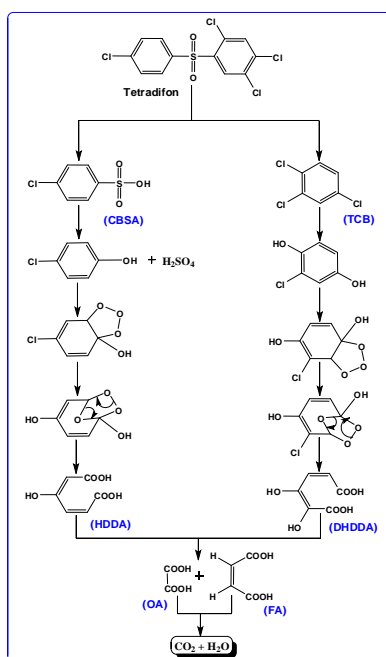
Figure 5s: (e) GC-MS Mass Spectrum of the CBSA



Figure 5s: (f) GC-MS Mass Spectrum of the HDDA

### 3.10. Reaction mechanism

Based on the observed experimental results, the probable mechanism for the photocatalysed degradation of tetradifon on Mn/TiO<sub>2</sub> in presence of ozone is proposed. In photocatalysed ozonation using heterogeneous catalyst, the photoinduced holes and electrons in semiconductor particles reportedly produce highly oxidizing species, which play a key role in degradation of organic pollutants [10]. The heterogeneous photocatalysed ozonation in the presence of metal oxides or metals/metal oxides on supports, the effectiveness of the catalytic process depends to an abundant scope on the properties of catalyst surface, which influence the properties of the surface active sites and photocatalysed ozone decomposition reactions in aqueous solutions. The most important chemical properties for the sustainable activity of catalyst are chemical stability and the presence of active surface sites, which are responsible for catalysed reactions [11].



**Proposed Mechanism: Mechanism of the Scheme**

It is well well-known that the electrophilic reactions of photolytic ozone take place on sites with strong electronic density. In particular, aromatics substituted with electron-withdrawing groups are highly reactive with photoinduced ozone electrons on carbons located in the ortho and para positions due to high electronic densities on these aromatic carbons whereas aromatics substituted with electron withdrawing groups (-SO<sub>2</sub>, -Cl) are weakly photolytically reactive. The molecular structure of tetradifon pesticide contains electron-withdrawing groups (-SO<sub>3</sub> and -Cl), hence photolytically ozone reactions should occur initially on certain preferential sites. In order to illustrate this, sites with strong electronic density were identified, and the analysis showed that it is likely that photocatalyzed ozone attack would take place at the sulfonyl group. Besides the electrophilic attack, ozone undergoes cycloaddition reaction with unsaturated bonds leads to the formation of compounds having the carbonyl group (-C=O) or the acid group (-COOH). With this in mind and in order to illustrate a possible reaction mechanism, further analysis was made with spectral analysis to identify the intermediate products. The spectral resulted in a number of compounds, which are shown in figure X. Based on, the sulfone compound, 4-chlorobenzenesulfonic acid (CBSA) and trichlorobenzene (TCB). According to this postulate that the bonds C-S and C-Cl in A and B are cleaved leading to the formation of another intermediates 4-chlorophenol and 2-chlorobenzene-1,4-diol. Further attacks of photoozone radicals leads to the conversion of 4-chlorophenol to 3-hydroxyhexa-2,4-dienedioic acid (HDDA), then to oxalic acid (OA) and also fumaric acid (FA), and eventually conversion to

mineralization (CO<sub>2</sub> and H<sub>2</sub>O). On the other hand, through cleavage of the C–Cl bond in compound trichlorobenzene (TCB) and with further photolytic ozone attack, dihydroxyhexa-2,4-dienedioic acid (DHDDA) is formed. Through further photolytic ozone attack, OA and FA are converted. Additionally, extended photolytic oxidation of the intermediates leads to complete mineralization to produce carbon dioxide and water (Scheme).

#### 4. Conclusions

Our study showed that the deposition-precipitation method permits the synthesis of Mn doped titania catalysts with good metal dispersion. The results of this study clearly indicate that Mn/TiO<sub>2</sub> can efficiently catalyze the degradation and mineralization of the tetradifon pesticide in the presence of light and ozone. The size of catalyst particles, and reaction parameters play a significant role in ozonolysis, so catalytic properties are strongly affected by the preparation method of the catalyst. Titania is a suitable support for loading of Mn catalysts. The tetradifon photooxidation was quantitative with 100% degradation. CBSA, TCB, HDDA and DHDDA were main products of which OA and FA were the secondary product, with partial mineralization. Photocatalysed ozonation is proved to be an effective method to remove chloro, sulfonyl and hydroxy groups from substituted organic pesticide.

#### ACKNOWLEDGEMENTS

The authors are thankful to the National Research Foundation of South Africa, University of KwaZulu-Natal, Durban, South Africa and Department of Chemistry, Annamacharya Institute of Technology & Sciences, Tirupati, India for providing facilities.

#### REFERENCES

1. Rissato S.R., Galhiane M.S., de Almeida M.V., Gerenutti M. and Apon B.M. (2007) Multiresidue determination of pesticides in honey samples by gas chromatography–mass spectrometry and application in environmental contamination. *Food Chem.*, **101(4)**, 1719–1726.
2. Field J.A and Sierra-Alvarez R. (2008) Microbial transformation and degradation of polychlorinated biphenyls. *Environ. Poll.*, **155(1)**, 1–12.
3. Legrini O., Oliveros E., and Braun A.M. (1993) Photochemical processes for water treatment. *Chem. Rev.* **93(2)**, 671–698.
4. Fathinia M., Khataee A., Naseri A and Aber A. (2015) Monitoring simultaneous photocatalytic-ozonation of mixture of pharmaceuticals in the presence of immobilized TiO<sub>2</sub> nanoparticles using MCR-ALS: Identification of intermediates and multi-response optimization approach. *Spectrochim. Acta Part A: Mol. & Biomol. Spectroscopy*, **136(C)**, 1275–1290.
5. Maddila S., Dasireddy V.D.B.C. and Jonnalagadda S.B. (2014). Ce-V loaded metal oxides as catalysts for dechlorination of chloronitrophenol by ozone. *Appl. Catal. B: Environ.* **150-151**, 305-314.
6. Maddila S., Oseghe E.O. and Jonnalagadda S.B. (2014). Photocatalysed ozonation by Ce doped TiO<sub>2</sub> catalyst degradation of pesticide, Dicamba in water. *J. Chem. Technol & Biotechnol.* DOI 10.1002/jctb.4583.
7. Maddila S., Lavanya P., and Jonnalagadda S.B (2014). Degradation, mineralization of bromoxynil pesticide by heterogeneous photocatalytic ozonation. *J. Indu. & Eng. Chem.* doi.org/10.1016/j.jiec.2014.10.005.
8. Maddila S., Dasireddy V.D.B.C and Jonnalagadda S.B. (2013). Dechlorination of tetrachloro-o-benzoquinone by ozonation catalyzed by cesium loaded metal oxides *Appl. Catal. B: Environ.* **138-139** 149-160.
9. Venieri D., Fraggadaki A., Kostadima M., Chatzisyneon E., Binas V., Zachopoulos A., Kiriakidis G and Mantzavinos D. (2014). Solar light and metal-doped TiO<sub>2</sub> to eliminate water-transmitted bacterial pathogens: Photocatalyst characterization and disinfection performance. *Appl. Catal. B: Environ.* **154–155**, 93–101.
10. Zhang W., Zou L., and Wang L. (2009). Photocatalytic TiO<sub>2</sub>/adsorbent nanocomposites prepared via wet chemical impregnation for wastewater treatment. *Appl. Catal. A: Gene.* **371(1-2)**, 1–9.
11. Kasprzyk-Hordern B., Ziolek M. and Nawrocki J. (2003). Catalytic ozonation and methods of enhancing molecular ozone reactions in water treatment. *Appl. Catal. B: Environ.* **46**, 639–669.